

Simple and Low-Cost Aerodynamic Drag Reduction Devices for Tractor-Trailer Trucks

Richard M. Wood
and

Steven X. S. Bauer
SOLUS – Solutions and Technologies

Copyright © 2003 SAE International

ABSTRACT

Three simple, low cost aerodynamic drag reduction devices have been developed for application to the trailer of a tractor-trailer truck. The three devices have undergone extensive operational testing where they have amassed over 85,000 miles of use. These technologies have shown a combined fuel savings of 10% at an average speed of 47.5 mph. This improvement in fuel economy correlates to an equivalent drag reduction of approximately 30% with a corresponding drag coefficient of 0.45. Observations and anecdotal evidence from the test activity have shown that the addition of these devices to the trailers has not had a negative impact on either the operational utility of the trailers or the maintenance procedures and requirements.

INTRODUCTION

An assessment of the energy usage of tractor-trailer trucks shows that the primary resistance forces are drive-train losses, rolling friction, and aerodynamic drag, see figure 1 [1, 2, 3]. The chart of figure 1 shows that as vehicle speed is increased the force required to overcome both aerodynamic drag and rolling friction increases. However, the rate of increase in aerodynamic drag with increasing vehicle speed is much greater than that for rolling friction such that at approximately 50 mph the force directed at overcoming aerodynamic drag exceeds that required to overcome rolling friction.

It should be noted that the graph shown in figure 1 is for the ideal case in which the vehicle is moving through undisturbed air [1, 2, 3]. These data do not take into account several operational and environmental factors that can have a dominating effect on the aerodynamic drag of tractor-trailer trucks [4, 5, 6, 7]. A more thorough accounting of all operational and environmental

concerns identifies a number of additional factors such as interference from other vehicles, atmospheric effects, and road conditions. All of these factors must be addressed when developing technologies to improve the fuel economy of heavy vehicles.

Shown in figure 2 is a schematic that depicts the impact of several of these operational and environmental based factors on the horsepower requirements of tractor-trailer trucks. The five factors listed at the top of figure 2 relate to the uncertainty of the aerodynamic load on a tractor-trailer truck. As noted in the figure, these factors all tend to increase the aerodynamic loading on a vehicle that has been designed based upon the ideal case represented in figure 1. In an operational environment these factors will vary continuously throughout the operational period and vary significantly with vehicle speed.

There are also a number of geometric factors that influence the aerodynamics of tractor-trailer trucks. Shown in figure 3 is the aerodynamic drag of tractor-trailer trucks due to changes in the flow field in the gap region between the tractor and trailer [8]. These data are for the ideal case of a vehicle operating at 60 mph in an undisturbed airflow. The data show that under ideal conditions a tractor-trailer truck in which the tractor has been designed to include aerodynamic shaping and has been fitted with roof and side fairings will have a drag coefficient between 0.6 and 0.7 whereas a tractor-trailer truck that does not have aerodynamic shaping and fairings will have a drag coefficient of 0.7 to 0.9.

The data of figure 3 can also be viewed as a summary of the aerodynamic drag reduction efforts for tractor-trailer vehicles over the past 20 to 30 years [1, 3, 4, 7 - 9 - 18]. The trucking community has focused on reducing the aerodynamic drag of the forward facing surfaces of both the tractor and trailer. Specifically, the aerodynamic drag has been reduced on the tractor forward facing surfaces through aerodynamic shaping of the tractor cab and the

aerodynamic drag has been reduced on the forward face of the trailer by adding aerodynamic fairings to the tractor in order to direct the flow away from the trailer front face. These efforts have produced reductions in the aerodynamic drag of 30%, for an operating speed of 60 mph, with corresponding improvements in fuel economy approaching 15%. However, these improvements have not been consistently realized under operational conditions [3, 4, 7, 12, 14, 19]. In an operational environment, the unsteady and erratic flow that the vehicle experiences degrades the effectiveness of these aerodynamic devices. An assessment of the aerodynamic drag in an operational environment indicates that the reduction in aerodynamic drag at 60 mph would be closer to 20%, which corresponds to a 10% improvement in fuel economy.

It is important to note that the drag reductions indicated above would drop significantly with a decrease in vehicle speed. The relationship between aerodynamic drag reduction, fuel economy, and vehicle speed is depicted in table 1 [1, 20, 21].

Vehicle Speed (mph)	Aerodynamic Drag Reduction to Increase Fuel Economy 1%
60	2%
40	3%
20	6%

Table 1. Relationship between aerodynamic-drag reduction and fuel economy improvement for tractor-trailer trucks.

The data presented in table 1 highlight the difficulty in achieving meaningful fuel savings of 10% for a typical tractor-trailer truck at an average speed below 60 mph. For an average speed of 40 mph the aerodynamic drag would have to be reduced 30% to achieve a fuel economy improvement of 10%. The chart also shows that if the average speed approaches 30 mph then it is nearly impossible to achieve a 10% improvement in fuel economy through aerodynamic drag reduction.

DISCUSSION

To better understand the technical challenge of drag reduction, it is important to understand the distribution of the drag between the tractor and trailer, see figure 4. The data used to develop the drag distributions depicted in figure 4 were obtained from a review of the data contained in references, 2 - 4, 7, 8, 12, 14, 15, and 17 - 19. These data show the relative magnitude of the aerodynamic drag force on a tractor-trailer truck under

ideal wind conditions. The schematic shows that the dominant drag regions on a tractor-trailer truck are the tractor front face, the gap region, and the trailer base. A review of the drag on a tractor-trailer truck, operating under ideal conditions, indicates that 40% to 50% of the aerodynamic drag is attributed to the tractor and 60% to 50% is attributed to the trailer. This variation in the drag distribution reflects the difference between a tractor with advanced aerodynamic shaping, roof-spoiler, and side-fairings, which would have a tractor-to-trailer drag distribution of 50% tractor drag and 50% trailer drag, whereas a tractor with minimal aerodynamic shaping and a more simplistic aerodynamic roof-spoiler and side-fairings would have a tractor-to-trailer drag distribution of 40% tractor drag and 60% trailer drag. However, the benefit of the aerodynamic fairing devices are not fully realized due to a variety of factors, most notably crosswind effects, see figure 5. As depicted in figure 5 the dominant drag areas on the vehicle are the same as those discussed in figure 4. Under operational conditions, the distribution of aerodynamic drag between the tractor and trailer remains at 40% for the tractor to 60% for the trailer for all tractor-trailer trucks, independent of the conventional aerodynamic enhancements. These observations indicate that a significant portion of the aerodynamic drag reduction gains made, with the addition of conventional aerodynamic fairings, is reduced under operational conditions.

All of the factors discussed above as well as numerous other issues should be viewed as constraints in the design of aerodynamic technologies that are directed at improving the fuel economy of tractor-trailer trucks. Additionally, design activities directed at improving the fuel efficiency of these vehicles must address vehicle operations, maintenance, safety, weight, and cost. Other vehicle performance factors that must also be addressed are aerodynamic loads, stability and handling, braking, splash and spray, and tire wear [2 - 7, 12, 19, 20].

AERODYNAMIC DESIGN

The objective of the aerodynamic drag reduction technology development activity was to design, develop, and demonstrate aerodynamic devices that would improve the fuel economy of tractor-trailer trucks under operational conditions. A further objective was to develop novel technologies and concepts. To ensure the unique nature of the technology under consideration for this activity, an extensive literature review was performed. A summary of this review is depicted in figure 6.

In pursuit of these goals, it was recognized that vehicle operations, maintenance, safety, weight, and cost would be primary constraints in the design. Additional vehicle

performance factors addressed in the design activity were aerodynamic loads, stability and handling, braking, splash and spray, and tire wear.

A mitigating factor in the design activity was the limitation of the experimental validation process available to the activity. The experimental validation portion of the activity was actually a demonstration activity in which the devices were to be installed on operational vehicles. A result of this approach was that testing would occur over an extended period of time and under diverse operational conditions. This is quite different from the traditional wind-tunnel test or SAE Type I or Type II processes in which the testing is performed in a controlled and focused manner and limited in scope in order to isolate various factors and variables in the test program. This operational based test approach resulted in fuel economy replacing aerodynamic drag as the figure of merit for the activity. The operational testing of the devices also required statistical analysis of the engine performance data to ensure an accurate assessment of the benefit of the aerodynamic device. Another issue that had to be addressed was the length of the test period. In order to obtain a statistically significant body of data, the test period was open ended. All of these factors required that the tested devices be designed to perform over a broad range of environmental and operational conditions. Furthermore the tested devices could not interfere with fleet operations or require additional maintenance.

The tractor-trailer trucks employed in this activity are used for regional delivery of lightweight goods. The tractors were late model International [22] day tractors with moderate aerodynamic shaping and were fitted with roof mounted aerodynamic deflectors and side fairings to control the gap flow and the flow over the trailer. The gap dimension was approximately 40.0 inches. The trailers were Great Dane [23] models that were identical in length, height, and width and had roll-up doors on the base. The operational data were obtained with the Cummins Engine INSITE Professional - SELECT Plus data acquisition and analysis system [24].

Because the aerodynamic drag reduction goal was difficult to quantify, the activity goal was defined as a 15% increase in fuel economy at 60 mph. A primary objective of the design activity was to develop a suite of technologies that would work together to not only increase fuel economy but to also improve vehicle safety. Shown in figure 7 are the three target areas selected for the design activity and the individual drag reduction goals for each target area. The design target areas are the gap region (A) (includes tractor base area and trailer front face), the trailer base area (B), and the trailer undercarriage (C). Also shown on the figure are the estimated initial and final aerodynamic drag values of the subject tractor-trailer truck. To achieve the fuel economy goal, the aerodynamic drag of the vehicle

would have to be reduced 30% at 60 mph. This drag reduction goal corresponds to a reduction in the tractor-trailer truck drag coefficient from 0.70 to a value of 0.50.

Design Approach

A knowledge based [25] design approach was used in the activity. This approach made use of existing published data and relied heavily upon the experience and knowledge of the authors. Numerous publications were reviewed to obtain insight into the complex flow environment and the operational constraints of the design space. Following are some of the noteworthy publications that were used; the work on trapped vortices [26 - 30], the work on boat tails [11, 14, 15, 31 - 35], the work on gap flows [10, 16, 36], the computational analysis detailing flow fields [20, 36 - 39], and reports providing design guidelines [3, 13, 14, 17, 18, 40]. The design activity was initiated with an extensive analysis of the data contained in the above referenced reports. This analysis identified several opportunities to explore the application of vortex flow technologies to the gap and base areas of the vehicle. To address the undercarriage flow and its interaction with the base flow, an undercarriage flow momentum enhancement technology was selected.

The aerodynamic design activity produced a number of concepts to meet the technical goals established for the activity. All concepts were designed as simple, fixed-geometry devices that neither required maintenance nor interfered with the operation and maintenance of the vehicles. All concepts were designed as add-on devices that attach to the outer surface or structure of the tractors or trailers. These concepts were reviewed with the owner and operator of the tractor-trailer vehicles to discuss a variety of issues including vehicle operations, maintenance, safety, weight, cost, aerodynamic loads, stability and handling, braking, splash and spray, and tire wear. Based upon these conversations three devices were selected for operational testing. The three selected devices were designed to mount on the trailers. These devices are referred to in the remainder of this report as; cross flow vortex trap device, vortex strake device, and undercarriage flow device.

Gap -Treatment Design

The design activity for the gap region focused on reducing the aerodynamic drag under crosswind conditions. As noted in figure 2, it is recognized that crosswind flow is always present in the operational environment of ground vehicles. A graphic of a typical tractor-trailer truck with a gap between the tractor and trailer is shown in figure 8. The graphic also depicts the flow streamlines that would be present if the truck was operating in the absence of a crosswind. To further

explore the complex gap flow environment, horizontal cross section cuts through the gap region are depicted in figures 9 and 10, for the condition of no crosswind and with a crosswind, respectively.

Figure 9 shows a graphic depicting the tractor and trailer geometry in the gap region and also the gap flow, for the condition of no crosswind. The schematic of the gap flow shows that a portion of the flow leaving the trailing edge of the tractor will separate at the tractor trailing edge and turn into the gap region. This inward turning flow impinges on the trailer front face resulting in an increase in pressure on the trailer front face and subsequent increase in aerodynamic drag. The presence of crosswind flow will tend to increase the flow volume and velocity that enters the gap region and impinges onto the trailer front face, see figure 10. This increased gap flow will tend to increase the pressure on the trailer front face compared to the no crosswind condition. An additional result of the flow expanding into the gap region is the reduction in pressure acting on the tractor base and thus an increase in aerodynamic drag on the tractor. Another detrimental effect of the crosswind flow entering the gap is the flow separation that occurs on the leeward side of the trailer producing a significant side force on the vehicle that may adversely affect the vehicle handling performance.

To reduce the aerodynamic drag associated with flow in the gap region, for both no crosswind and crosswind flow conditions, an aerodynamic design was conducted using existing published data. The design principle is based upon trapped vortex technology in which a region on a vehicle is constructed to capture or trap a vortex that is formed when the incident flow encounters an aerodynamically sharp edge. In the present design activity, a vortex-trap device was designed and located on the forward facing front face of the trailer. The subject, patent pending, device is termed the Cross-flow Vortex Trap Device (CVTD). The leading edge of the adjacent surfaces comprising the CVTD were made aerodynamically sharp to ensure that the gap flow will separate at the leading edge of each adjacent surface and generate a vortex that is trapped between adjacent surfaces comprising the CVTD. Each trapped vortex imparts a low pressure on the forward facing surface of the trailer.

Depicted in figure 11 is a sketch of a six surface CVTD installed on or integrated into the front face of a trailer. A photograph of the prototype CVTD installed on the test vehicle is shown in figure 12. The prototype CVTD consisted of seven, duplicate, equally spaced, vertically aligned, and adjacent planar surfaces. Each surface of the prototype CVTD extended perpendicular from the surface of the trailer, was 12 inches wide with each surface extending vertically over a substantial portion of the trailer front face.

A sketch of the CVTD induced flow characteristics are depicted in figure 13. The sketch shows the expected gap flow and CVTD flow characteristics for a minimal, left to right crosswind. Note, the sketch of figure 13 is for a six surface CVTD. The figure shows the same initial gap flow features as those depicted in figure 10. As the gap cross flow develops it encounters the leading edge of the furthest windward CVTD surface. The gap cross flow separates at the leading edge of the furthest windward CVTD and forms a vortex that is trapped between the furthest windward surface and the adjacent surface, located immediately inboard. The flow separation at the leading edge of the CVTD induces an acceleration of the flow located immediately forward of the CVTD. This induced flow field is accelerated toward the leading edge of the adjacent surface. These flow characteristics are repeated at each subsequent surface, moving from left to right.

The velocity in the trapped-vortex is significantly greater than the surrounding flow thereby producing low pressure that acts on both of the adjacent surfaces of the CVTD and the trailer front face. The pressure loadings on adjacent surfaces of the CVTD are orientated perpendicular to the vehicle axis and thereby they do not contribute the vehicle aerodynamic drag force. The force on the adjacent surfaces are also equal and opposite and do not contribute to the side force on the vehicle. However, the trapped vortices generate low pressures that act on the trailer front face and these pressures generate a force that is aligned with the vehicle longitudinal axis. The low pressures induced by the trapped vortex reduce the aerodynamic drag of the vehicle and if the trapped vortices are of sufficient strength the resultant force may become an aerodynamic thrust force.

Trailer Base and Undercarriage Design

The design effort directed at the trailer base and trailer undercarriage was developed in an integrated fashion in order to ensure that both concepts contributed to the base area drag reduction in addition to the undercarriage and aft wheel drag reduction. A graphic of a typical trailer aft end region is shown in figure 14. In the design activity it was recognized that the base and undercarriage concepts must be applicable to a variety of door types (e.g., roll-up and swing open) and must apply to all longitudinal positions of the aft wheel set. The technical challenge was to control the massively separated and unsteady wake behind the bluff base area, see figure 15. The schematics of figure 15 show top and side views of the dominant wake flow features behind a tractor-trailer truck. The top view shows that the wake is comprised of different shape and size vortex structures that vary in direction of rotation. These rotational structures result from the low energy flow passing along the sides and top of the trailer that separates at the trailing edge of the

trailer and spills into the trailer base area. This base area flow interacts with the low energy flow exiting from under the trailer resulting in an even greater unsteady flow environment.

To improve the base flow characteristics and reduce the aerodynamic drag of the vehicle two aerodynamic devices were designed and tested. The first of these, patent pending, devices is termed the Vortex Strake Device (VSD). As shown in figure 16, the VSD is attached to or integrated into the side and top surfaces of the trailer near the vehicle trailing edge. A photograph of the prototype VSD installed on the test trailer is shown in figure 17. The prototype VSD consisted of five, duplicate, equally spaced and aligned, adjacent planar panels on each side of the trailer. In addition, four duplicate panels were located on the top surface of the trailer in a chevron pattern as shown in figure 16. Each panel, comprising the prototype VSD, was 36 inches long and 2 inches in width. Each VSD panel, on the sides of the vehicle, was inclined 30°, leading edge up. Each VSD panel, on the roof of the vehicle, was inclined 30°, leading edge inboard.

A sketch of the VSD induced flow characteristics are depicted in figure 18. The sketch shows the expected VSD flow characteristics for all free-stream flow conditions. Note, the sketch of figure 18 shows a VSD with four panels on each side surface and four panels on the top surface. The VSD generates a limited number of large vortex structures generated on the side and top exterior surfaces of a trailer to energize the flow exiting the trailing edge of the side and top exterior surfaces of the trailer, thereby increasing the ability of the flow on the trailer side and trailer top exterior surfaces to expand into the base region and provide drag reduction, increased fuel economy and improved operational performance. To maximize the ability of each of the VSD panels to generate a coherent vortex structure, the panels are aligned in planes or surfaces that are perpendicular to the surface of the vehicle. The vortices generated by the VSD are symmetrically orientated about the centerline of the trailer. The subject vortices have a preferred angular velocity and direction that enhances the mixing of the trailer undercarriage flow with the bluff-base wake flow. The result is a stable bluff-base wake flow and a high pressure that acts on the base surface of the trailer. The strength of the vortices formed by the VSD and thus, the aerodynamic drag reduction benefit, increase with increasing flow velocity.

The second, patent pending, device to improve the base flow characteristics and reduce the aerodynamic drag of the vehicle is termed the Undercarriage Flow Device (UFD). As shown in figure 19, the UFD is attached to the lower surface of the trailer near the vehicle trailing edge. The UFD acts as a convergent duct and consists of specifically designed aerodynamically contoured surfaces that are positioned under a vehicle

with its minimum opening located at the base of a blunt based ground vehicle and its maximum opening located upstream of the minimum opening. The UFD is designed to change the low momentum under-carriage flow into a coherent high momentum flow. A photograph of the prototype UFD installed on the test trailer is shown in figure 20. The prototype UFD consisted of two opposing surfaces located symmetrically about the vehicle centerline. Each surface, comprising the prototype UFD, extended from just aft of the rear wheel, forward 45 inches, inboard 39 inches and extended from the vehicle lower surface 40 inches towards the ground. Each surface of the prototype was aerodynamically contoured to minimize local flow separation on the inward and outward facing sides of the surface.

A sketch of the UFD induced flow characteristics are depicted in figure 21. The sketch shows the expected UFD flow features for all free-stream flow conditions. The aerodynamically contoured UFD surfaces collect the undercarriage flow, downstream of the most aft set of wheels, and accelerate the flow into the bluff-base wake, thus increasing the base pressure and lowering base drag. The high momentum flow produced by the UFD generates a counter-rotating vortex structure that vertically displaces the primary wake vortex. This new vortex structure energizes the existing vortex flow and adds energy and stability to the wake flow. The combination of the two vortex structures creates a fluidic boat tail that reduces the turning required by the side and top flows and results in an increase in pressure in the wake and on the bluff-base area. The increased base pressure results in a reduction in aerodynamic drag.

OPERATIONAL TESTING

The intent of the operational test program was to minimize the large number of factors that influence fuel economy, such as type and geometry of the tractors and trailers, the operational routes, the loads carried by the vehicles, operator behavior, fuel quality, tire quality, rolling friction, and environmental concerns to name a few. A detailed list of these factors is provided in figure 22. Of greater importance to the fleet owner was the impact on operations and maintenance requirements.

The test program was structured to evaluate each of the three patent-pending devices individually. The test program included the operation of matching baseline trailer (i.e., no device installed) for each of the experimental trailers. The baseline and experimental trailers were to be pulled by the same tractor, which alternated between the two trailers. Each of the baseline and experimental trailer pairs were to be pulled over the same route. However, each trailer pair (i.e., experimental device) was pulled on a different route and thus, each device experienced different environmental and road conditions. Another variable considered in the test activity was the effect that the style/model of the tractor

had on the results. The fleet owner had three different style/model tractors that needed to be integrated in to the test activity. However, due to the concern of impacting fleet operation the organization and management of these variables was at the discretion of the fleet owner.

The fleet owner minimized fuel related factors by ensuring that each tractor received fuel from the fleet owners fuel supply system and by using the same fuel fill procedures for all test data runs. To minimize the affect of tires the fleet owner ensured that each tractor and trailer involved in the test had similar tire types and tread depth.

The collection and delivery of the engine / tractor performance data was the responsibility of the fleet owner. The fleet owner relied upon the Cummins engine INSITE professional CELECT Plus data acquisition and analysis software [24]. The data were to be collected on a daily basis and provided to the engineering team for analysis. A typical data sheet for a single test period is shown in table 2. The data sheet shows both a running total for the tractor as well as performance information for the most recent trip period. For the data shown in table 2, the trip time was 16.4 hours and the trip length was 762.8 miles. The data sheet also shows a trip idle time of 1.0 hour. These numbers correspond to an average speed of 47.4 mph with 6.2% of the time spent at idle. After a review of all of the data, it was determined that average speed and percent idle time would be two criteria that will be used to determine the usefulness of the data. For this investigation, any trip data that showed average speeds below 40 mph or idle times above 15% would not be used in the analysis.

Summary of Operational Testing

Operational performance data have been obtained on a fleet of tractor-trailer trucks that have been out-fitted with three patent-pending aerodynamic drag reduction technologies. The data collection period extended from July 2001 to March 2003. The testing was performed in which duplicate trailers were operated with and without the aerodynamic drag reduction technologies. Each matched set of trailers was operated over a limited number of routes. To evaluate the impact of variation in tractors, each baseline trailer and experimental trailer, comprising the matched set, was pulled by each of the three tractor types operated by the fleet.

Listed below is a summary of the data obtained.

Dates of Operational Testing - July 2001 to March 2002 and July 2002 and March 2003,

Total Trips	232
Total Miles	253600
Baseline Trailer Trips	135
Baseline Trailer Miles	143207
Experimental Trailer Trips	97
Experimental Trailer Miles	110393
Available Trips	155
Available Miles	182494
Baseline Trailer Trips	86
Baseline Trailer Miles	97165
Baseline Trailer Avg. Speed	47.8
Experimental Trailer Trips	69
Experimental Trailer Miles	85329
Experimental Trailer Avg. Speed	47.4

The average speed of each data set was approximately 47.5 miles per hour.

Analysis of Operational Data

As discussed previously, there are a large number of factors that influence the fuel economy of tractor-trailer trucks. A listing of a number of these factors is contained in figure 22 in which there are four main categories identified; aerodynamics, engine and drive train, environment, tires, and operations. In the present operational test it was recognized that each of these areas influence the fuel economy by more than 10%. It was further recognized that it is not possible to control or even document a significant number of these factors. As a result, it was determined that the only means available to the authors to account for the known variability in the data was to increase the number of data points. This approach required that the testing to occur over two, nine-month time periods. The three-month break in the testing between April and June of 2002 was used to evaluate progress and to improve the data acquisition process. This extended test period resulted in environmental factors influencing the data. A review of data from the National Oceanographic and Atmospheric Administration (NOAA) [41] revealed that the yearly temperature variation in the geographical location of the truck operations was greater than 50°. A plot of the average monthly daylight temperature data, for the time period of testing, is presented in figure 23. It is estimated that the 50° variation in temperature could influence the data by more than 6%.

To review the quality of data obtained in the test and to evaluate the effect of temperature changes, all data from the operational testing are plotted as a function of the date obtained, see figures 24, 25, and 26. Figure 24 shows fuel economy data for the baseline trailers as a function of month. Also shown in the figure is a 2nd order polynomial curve fit of the data. This curve fit was used to evaluate the general trend of the data with time. The curve-fit shows a variation of 10% between the winter and summer average monthly data. However, the raw data show a large scatter with a maximum variation of 18% in a single month time period. This variation in data is easily understandable based upon the large number of factors that could not be controlled in the test process. To determine the significance of the data scatter, a review of published data, for controlled testing, showed variations on the order of 5% can occur [40].

To provide additional analysis of the baseline data results for each of the three tractors used in the test program are presented in figure 25a, b, and c. As with the data of figure 24 a 2nd-order polynomial curve fit of the data is also presented in the figure. The data for an individual tractor show a reduced scatter in a single month, compared to the data of figure 24. Tractors B and C have the largest variation in a single month, on the order of 10%. The curve fit for each tractor shows a similar trend as that of figure 24 with a variation in fuel economy between winter and summer months of 5 to 10%. Although significant scatter remains, it is encouraging that the scatter in the data of figure 25 does compare favorably to published fuel economy data variations [40].

The raw data obtained on the three aerodynamic drag reduction devices are presented in figure 26a, b, and c. The data are presented in the same format as the data for the baseline trailers in figures 24 and 25. Note, the raw data of figure 26 are for each tractor, however, the curve fit is for all of the data for a specific aerodynamic drag reduction device. A review of the data in figure 26 show that the largest data scatter, for a given tractor, in a single month is less than 10% and the average scatter for a given tractor is approximately 5%. The 5% scatter in the data for a single tractor is equivalent to previously published data [40]. The data of figure 26 show that the most consistent and largest variation in the data is due to temperature, as indicated by date. The curve fit of figures 26a, b, and c show a consistent 12% variation between winter and summer months. A comparison of the curve fit data for the three drag reduction devices, figure 26, to the curve fit data for the baseline trailers, figure 24 and 25, show that the drag reduction devices provide increased fuel economy. A more detailed analysis of the fuel efficiency improvements is presented in figures 27, 28, and 29.

The data of figures 27, 28, and 29 are summary analysis results showing the changes in fuel economy due to the addition of the aerodynamic drag reduction devices. The

data of figure 27 are average fuel economy results as a function of each tractor, figure 28 show average fuel economy results as a function of daytime temperature, and figure 29 is a summary of five different averaging methods.

The results presented in figure 27 were derived by differencing the data, for the baseline trailers and the trailers with the drag-reduction device installed, for a given tractor. The data presented on the right of the figure are an average change in fuel economy for all tractors. The figure shows that all of the change in fuel economy values are positive with the exception of the VSD on tractor A and the UFD on tractor C. Comparing the change in fuel economy between the three devices show that the largest change was 10% on tractor A and the smallest change was 5% on tractor B. The cause of the variation is not understood. The variation in the change in fuel economy with a change in tractor was not unexpected based upon the variation in the raw data discussed previously. The average fuel economy improvement for all tractors was approximately 5 % for the CVTD and near 1% for both the VSD and UFD.

Presented in figure 28 is the effect of temperature on the change in fuel economy provided by the three drag reduction devices. Fuel economy improvements for each device have been calculated for temperatures less than 45°, temperatures between 45° and 75°, and for temperatures greater than 75°. Another way to view the data of figure 28 is that it represents a differencing of the 2nd-order curve fits of figure 26 from the curve fit of figure 24. The data presented on the right of the graph are an average change in fuel economy for all temperature ranges. The data show that all values are positive with the exception of the UFD for temperatures less than 45°. Comparing the change in fuel economy between the three devices shows that the largest change was 3.5% for temperature between 45° and 75° and the smallest change was 1% for temperatures greater than 75°. A comparison of these data to the tractor-based analysis of figure 27 shows that the temperature-based data has less variation indicating that temperature is a more consistent and predictable influence on the data. The average fuel economy improvement for all tractors was approximately 3.6 % for both the CVTD and the VSD and 2% for the UFD.

A summary of all of the data analysis is presented in figure 29 where the results for five separate averaging schemes are depicted for each of the three drag reduction devices. The fuel economy improvement values presented are; arithmetic mean average, average based upon tractor (see right side of figure 27), average based upon tractor and weighted by miles, average based upon temperature (see right side of figure 28), and average based upon temperature weighted by miles. The purpose of weighting the data by miles is to ensure that a low mileage data point did not have equal

weight as a high mileage data point. Note, the figure shows positive increases in fuel economy for all averaging approaches. The data show that the CVTD has the largest fuel economy improvement followed by the VSD and the UFD. All three devices have been designed to work in concert with one another and therefore, it is assumed that the integrated benefit of these devices to a tractor-trailer truck can be estimated by a simple addition of the individual contributions. Listed below is the range of fuel economy improvement values for each device and for the integrated benefit of all devices. Note, the integrated values reflect the summation of benefits for a straight average (6.5) and for average based upon temperature weighted by miles (16.5).

Device	Improvement in Fuel Economy (%)
CVTD	3.5 to 8.3
UFD	0.8 to 3.3
VSD	2.2 to 4.9
TOTAL	6.5 to 16.5

CONCLUDING REMARKS

Reported herein was a preliminary review of an ongoing tractor-trailer truck fuel economy improvement activity. The subject activity was an aerodynamic drag reduction effort in which low cost, simple, geometric devices are designed and validated through operational testing. To date, three aerodynamic drag reduction devices have been developed for application to the trailer of a tractor-trailer truck. The three devices have undergone extensive operational testing where they have amassed over 85,000 miles of use. These technologies have shown a combined fuel savings of approximately 10% at an average speed of 47.5 mph. This improvement in fuel economy correlates to an equivalent drag reduction of approximately 30% with a corresponding drag coefficient of 0.45. Note, the aerodynamic drag reduction and associated fuel savings also result in a measurable reduction in exhaust emissions that is equivalent to the percent reduction in fuel usage.

Observations from the test activity have shown that the addition of these devices to the trailers has not had a negative impact on either the operational utility of the trailers or the maintenance procedures and requirements. Anecdotal evidence indicates that these devices have not altered any of the vehicle driving and handling characteristics.

The application of the subject aerodynamic drag reduction technologies to trucks and similar high drag vehicles offers additional synergistic benefits such as the

ability to use of alternate lower-energy fuels and the use of alternate power sources.

REFERENCES

1. Hoerner, S. F.: Fluid Dynamic Drag. 1965
2. Blau, P. J.: Energy Efficiency in Heavy Vehicle Tires, Drivetrains and Braking Systems. Oak Ridge National Lab, OHVT, DOE. April 26, 2000.
3. Hucho, W. H.: Aerodynamics of Road Vehicles. Fourth Ed., pp. 415-488, 1988.
4. Drollinger, R. A.: Heavy Duty Truck Aerodynamics. SAE 870001, 1987.
5. Multiyear Program Plan for 1998-2002. Office of Heavy Vehicle Technology and Heavy Vehicle Industry Partners. DOE/ORO-2071, Aug. 1998.
6. A Multi-Year Program Plan for the Aerodynamic Design of Heavy Vehicles. <http://enr.gov/aerodrag/>
7. Drollinger, R. A.: Heavy Duty Truck Aerodynamics. SAE 870001, SP-688.
8. Sovran, G. et al: Aerodynamic Drag Mechanisms of Bluff Bodies and Road Vehicles. Plenum Publishing Corp., 1978.
9. SAE Wind Tunnel Test Procedure for Trucks and Buses. SAE J1252, July 1981, SAE Recommended Practice, 1981.
10. Saltzman, E. J. and Meyer, R. R. Jr.: Drag Reduction Obtained by Rounding Vertical Corners on a Box-Shaped Ground Vehicle. NASA TM X-56023, March 1974.
11. Saltzman, E. J., Meyer, R. R. Jr. and Lux, D. P.: Drag Reduction Obtained by Modifying a Box-Shaped Ground Vehicle. NASA TM X-56027, Oct. 1974.
12. Tyrrell, C. L.: Aerodynamics and Fuel Economy On Highway Experience. SAE 872278, 1987.
13. Barnard, R. H.: Road Vehicles Aerodynamic Design. Pp. 1-49, 1986.
14. Cooper, K. R.: The Effect of Front-Edge Rounding and Rear-Edge Shaping on the Aerodynamic Drag of Bluff Bodies. SAE 850288, 1985.
15. Sherwood, A. W.: Wind Tunnel Test of Trailmobile Trailers, 2nd Series, University of Maryland Wind Tunnel Report No. 85, College Park, MD, April 1974.
16. Bauer, P. T. and Sevaris, R. A.: An Experimental and Analytical Investigation of Truck Aerodynamics. Proc. Of the Conference/Workshop on the Reduction of the Aerodynamic Drag of Trucks. California Institute of Technology, Oct. 10-11, NSF RANN Doc Center, Wash. D. C. pp. 55-61.
17. Cooper, K. R.: Commercial Vehicle Aerodynamic Drag Reduction: Historical Perspective as a Guide. Proc. Of UEF Conference, Dec. 2-6, 2002. The Aerodynamics of Heavy Vehicles: Trucks, Buses and Trains.
18. Ehlbeck, J. M. and Mayenburg, M.: Increasing Heavy-Duty Fuel Economy. SAE 912662, 1991.

19. McCallen, R. et al.: Progress in Reducing Aerodynamic Drag for Higher Efficiency Heavy-Duty Trucks (Class 7 and 8). SAE 1999-01-2238, 1999.
20. Himeno, R., Fujitan, K., Nishikawa, J., Watanabe, Y., and Michitoshi, T.: Practical Economic Aspects of Tractor/Trailer Aerodynamics. SAE 760103, 1976.
21. Lachman, G. V.: Boundary Layer and Flow Control. Vol. I Pergamon Press, N. Y., 1961.
22. International Truck and Engine; <http://www.internationaldelivers.com>
23. Great Dane Trailers; <http://www.greatdanetrailers.com>
24. Cummins Engine; <http://www.cummins.com>
25. Wood, R. M. and Bauer, S. X. S.: A Discussion of Knowledge Based Design. AIAA Journal of Aircraft Vol. 40, No. 1, Jan-Feb 2003.
26. Rossow, V. J.: Lift Enhancement by an Externally Trapped Vortex. J. of Aircraft, Vol. 15, No. 9, Sept. 1978, pp. 618-625.
27. Rossow, V. J.: Two-Fence Concept for Efficient Trapping of Vortices on Airfoils. J. of Aircraft, Vol. 29, No. 5, Sept.-Oct. 1992, pp. 847-855.
28. Garcia, D. L. and Katz, J.: Trapped-Vortex in Ground Effect. AIAA 2002-3307, June 2002.
29. Cornish, J. J. III: Trapped Vortex Flow Control for Automobiles. Proc. Of the Second AIAA Symposia on Aerodynamics of Sports and Competition Autos, Bernard Pub., ed. May 1974, pp. 111-118.
30. Tanner, M.: New Investigation for Reducing the Base Drag of Wings with Blunt Trailing Edges. Aerodynamic Drag, AGARD-CP-124, Apr. 1973, pp. 121-129.
31. Saltzman, E. J.: A Summary of NASA Dryden's Truck Aerodynamic Research. SAE Paper 82184, Truck and Bus Meeting and Exposition, 1982.
32. Peterson, R. L.: Drag Reduction Obtained by the Addition of a Boattail to a Box-Shaped Vehicle. NASA CR-163113, Aug. 1981.
33. Lanser, W. R., Ross, J. C. and Kaufman, A. E.: Aerodynamic Performance of a Drag Reduction Device on a Full-Scale Tractor Trailer. SAE 912125.
34. Gutierrez, W. T., Hassan, B. Croll, R. H. and Rutledge, W. H.: Aerodynamic Overview of the Ground Transportation Systems (GTS) Project for Heavy Vehicle Drag Reduction. SAE 960906, SP-1145, 1996.
35. Muirhead, V. U.: An Investigation of Drag Reduction for Tractor Trailer Vehicles with Air Deflectors and Boattail. NASA CR-163104, 1981.
36. Nakamura, S., Hively, E. M. and Conlisk, A. T.: LES Simulation of Aerodynamic Drag for Heavy Duty Trailer Trucks. Proc. Of the ASME Fluids Engineering Division Summer Meeting. FEDSM 2002-31427, July 2002.
37. Roy, S. and Srinivasan, P.: External Flow Analysis of a Truck for Drag Reduction. SAE 2000-01-3500, 2000.
38. McCallen, R. et. Al.: March 2001 Working Group Meeting on Heavy Vehicle Aerodynamic Drag: Presentations and Summary Comments and Conclusions. UCRL-ID-143848, May 2001.
39. Bayraktar, I. and Baysal, O.: Computational Parametric Study on External Aerodynamics of Heavy Trucks. Proc. Of UEF 2002 The Aerodynamics of Heavy vehicles: Trucks, Buses and Trains, Dec. 2-6, 2002.
40. White Paper on Fuel Economy. Kenworth Truck Company, Oct. 2001, http://www.kenworth.com/The_Dynamics_of_Fuel_Efficiency.pdf
41. National Oceanographic and Atmospheric Administration. www.noaa.gov

CONTACT

Richard M. Wood and Steven Bauer

SOLUS-Solutions and Technologies

solutions@solusinc.com

DEFINITIONS, ACRONYMS, ABBREVIATIONS

A	maximum cross sectional area of tractor-trailer vehicle, ft ²
C _D	drag coefficient, D/AQ
d	equivalent diameter based upon A, ft.
D	aerodynamic drag force, lbs.
G	gap between tractor and trailer, ft.
HP	horsepower
mpg	miles per gallon
mph	miles per hour
psf	pounds per square foot
Q	dynamic pressure, psf
V	vehicle speed, mph

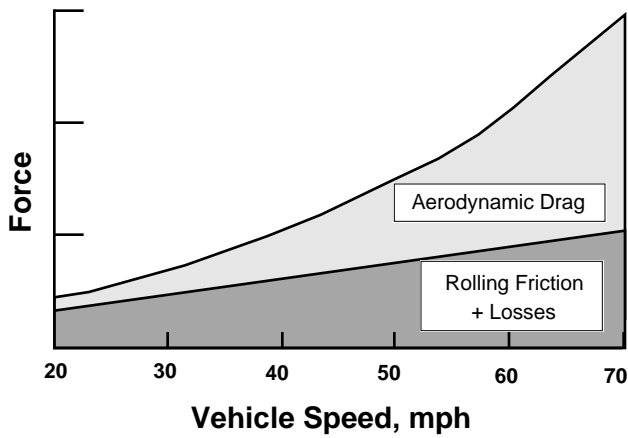


Figure 1. Graphic depicting representative horsepower requirements versus vehicle speed for a heavy vehicle tractor-trailer truck.

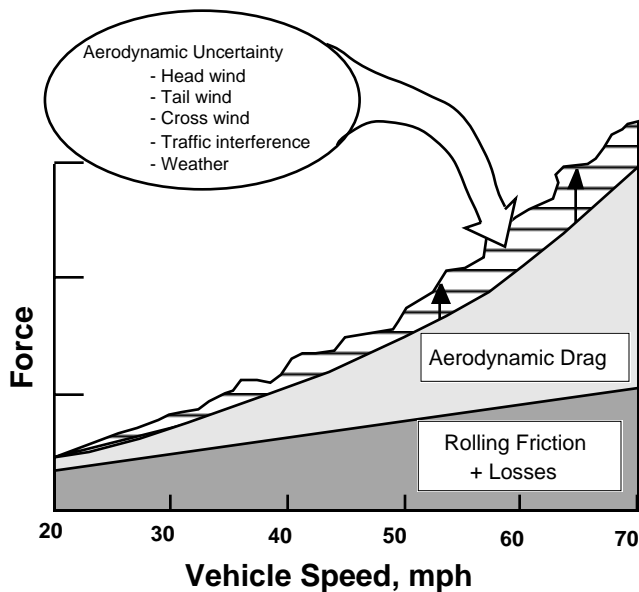


Figure 2. Graphic depicting the impact of aerodynamic uncertainty on horsepower requirements for a heavy vehicle tractor-trailer truck.

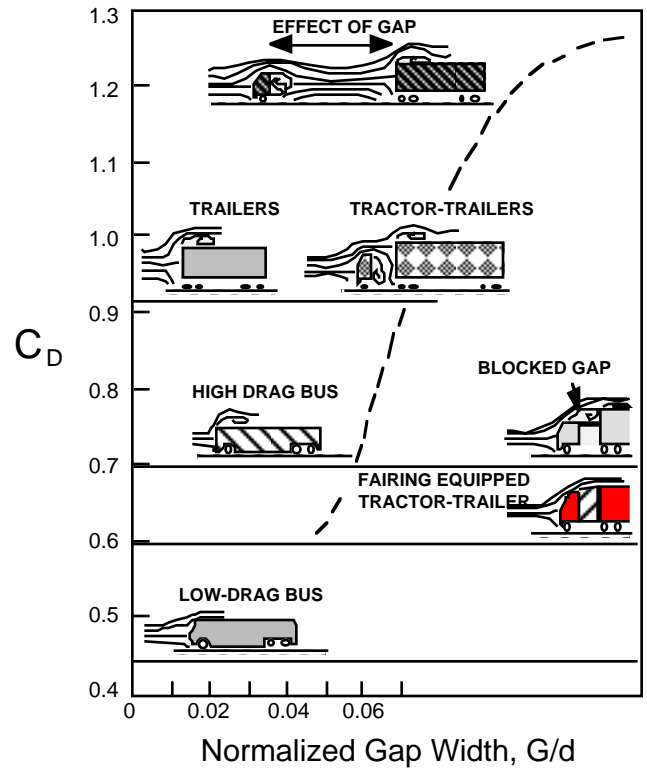


Figure 3. Aerodynamic drag on heavy vehicles as a function of gap width [3].

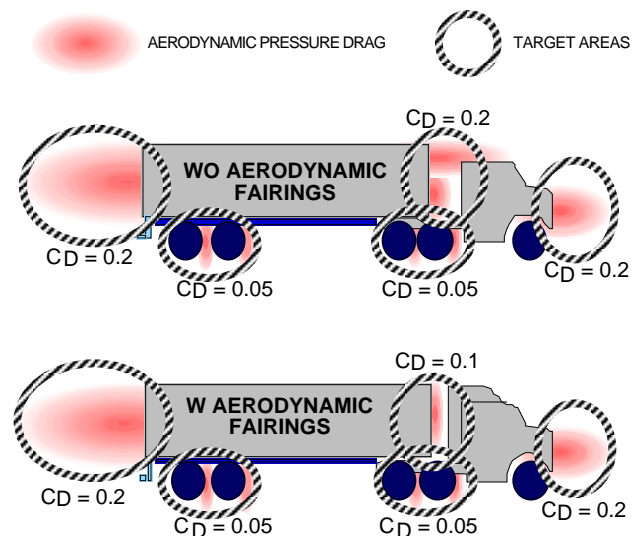


Figure 4. Graphic depicting the distribution of aerodynamic drag for a heavy vehicle tractor-trailer truck, with and without aerodynamic fairings, operating in a zero crosswind condition.

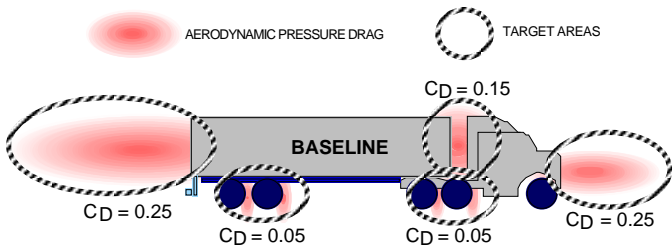


Figure 5. Graphic depicting the distribution of aerodynamic drag for a heavy vehicle tractor-trailer truck with aerodynamic fairings operating in a crosswind.

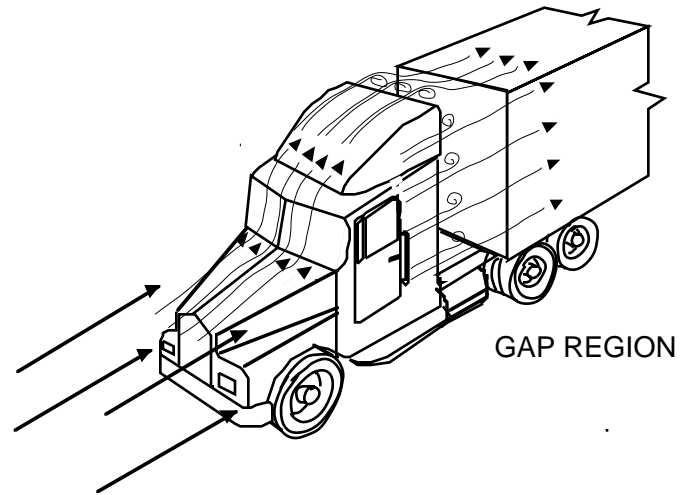


Figure 8. Graphic depicting the gap region for a typical tractor-trailer truck

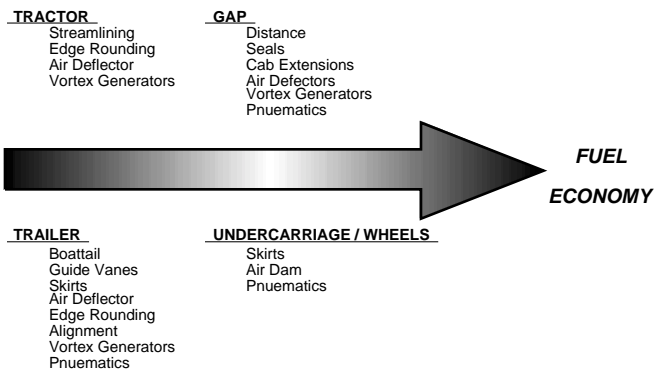


Figure 6. Graphic depicting the factors influencing aerodynamic drag for heavy vehicle tractor-trailer truck

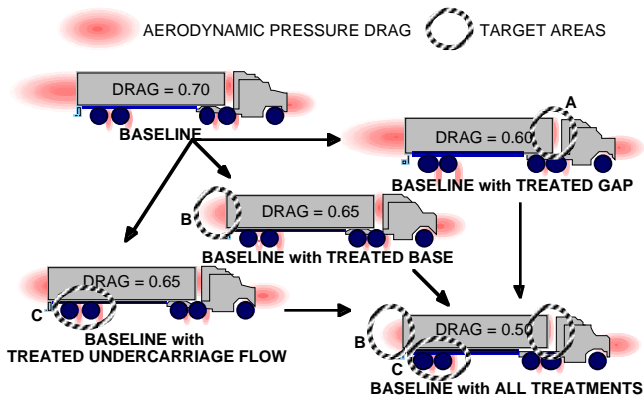


Figure 7. Graphic depicting the design target areas and drag reduction goals established for the activity.

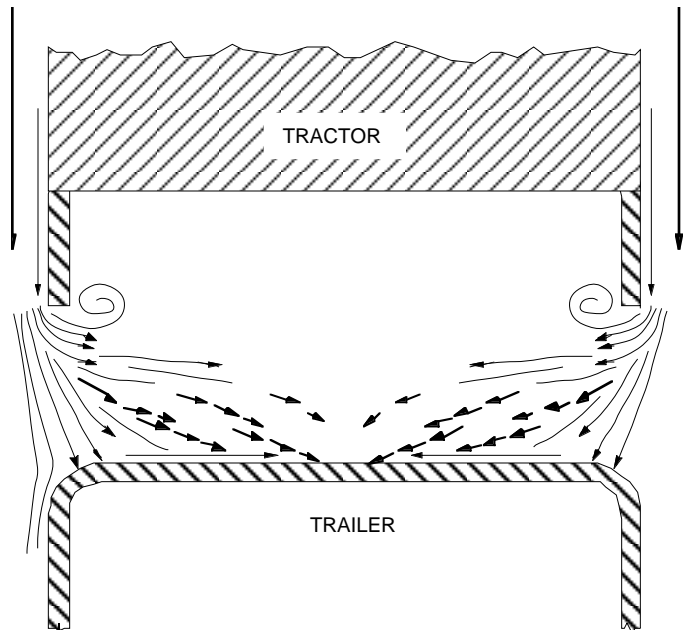


Figure 9. Sketch of the gap flow characteristics for a typical tractor-trailer truck operating with zero cross wind.

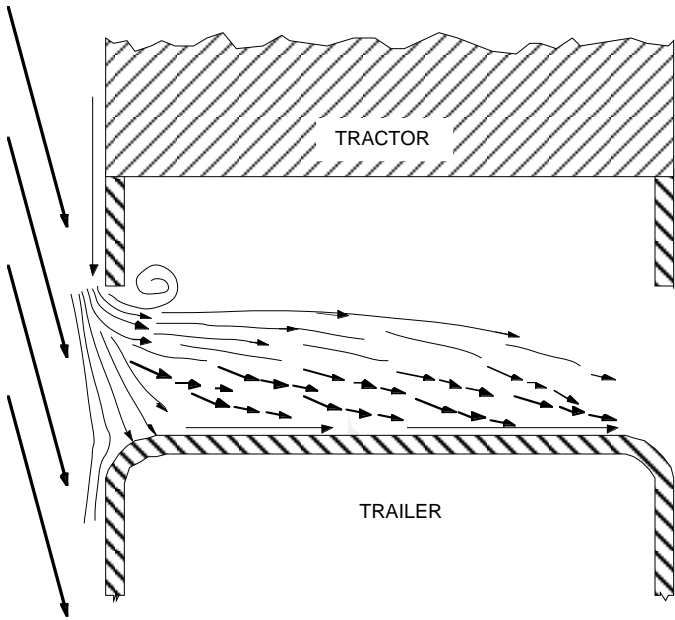
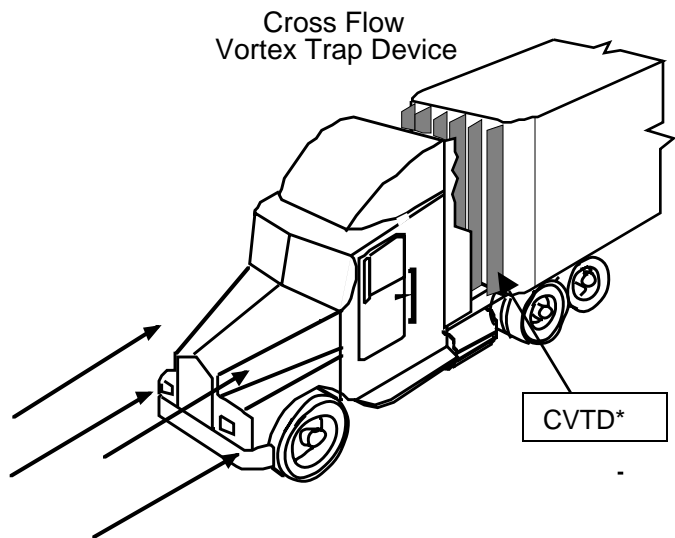


Figure 10. Sketch of the gap flow characteristics for a typical tractor-trailer truck operating in a cross wind.



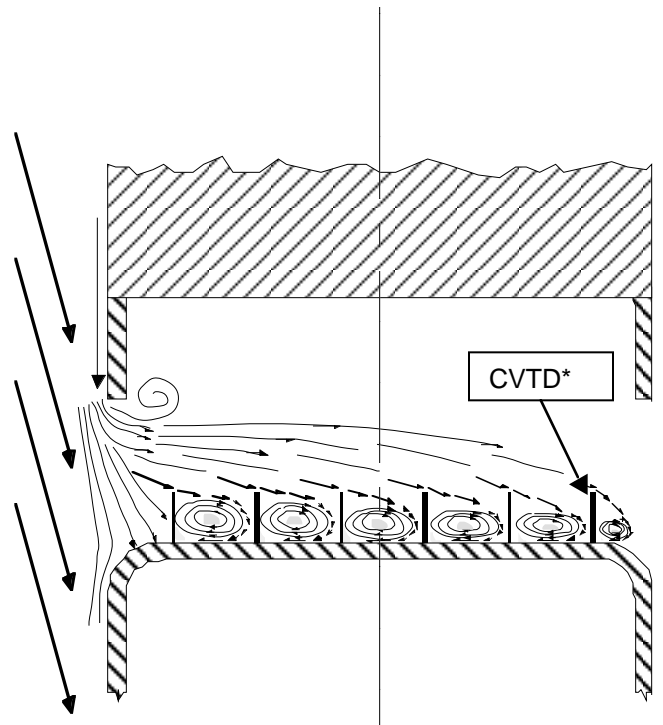
***PATENT PENDING**

Figure 12. Photograph of the cross flow vortex trap gap treatment device installed on the trailer front face.



***PATENT PENDING**

Figure 11. Sketch of the cross flow vortex trap gap treatment device installed on the trailer front face.



***PATENT PENDING**

Figure 13. Sketch of the cross flow vortex trap gap flow characteristics for a typical tractor-trailer truck operating in a cross wind with the gap treatment installed.

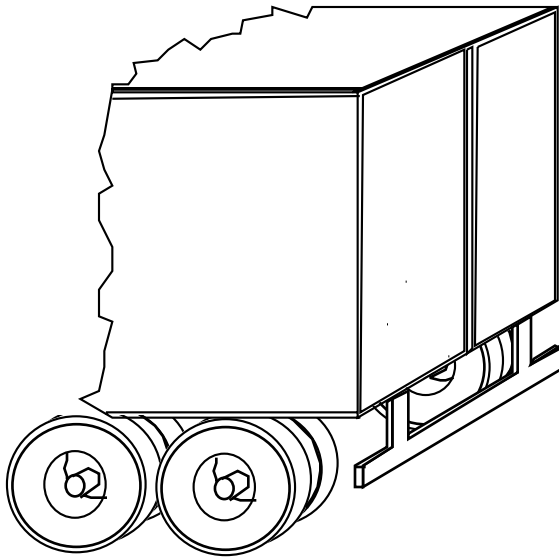
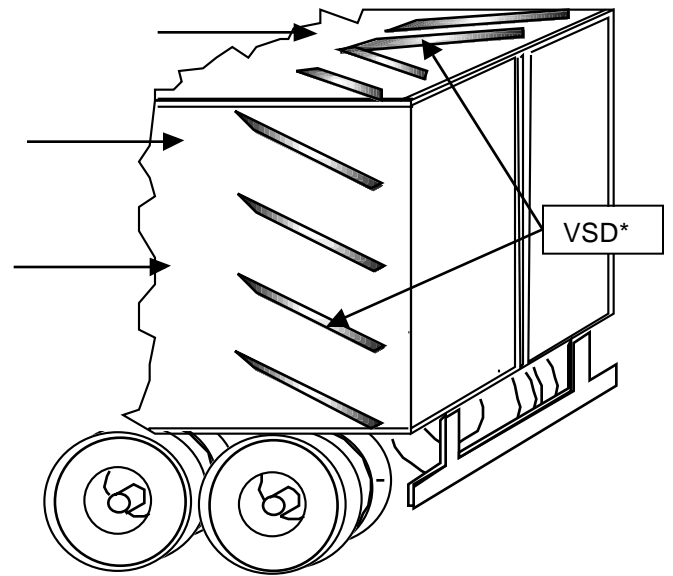


Figure 14. Graphic depicting the trailer bluff base and aft wheel set of a tractor-trailer truck.



***PATENT PENDING**

Figure 16. Sketch of the vortex strake trailer base treatment device installed on the aft portion of the trailer.

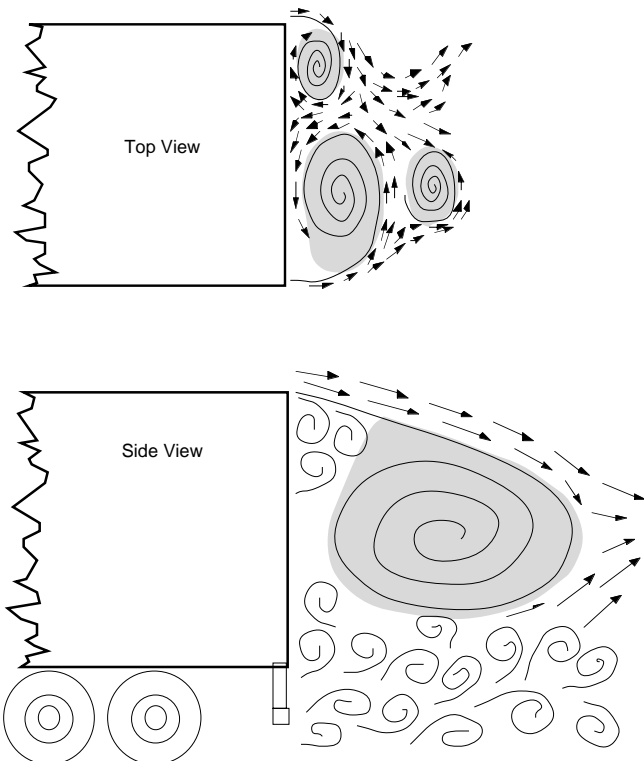
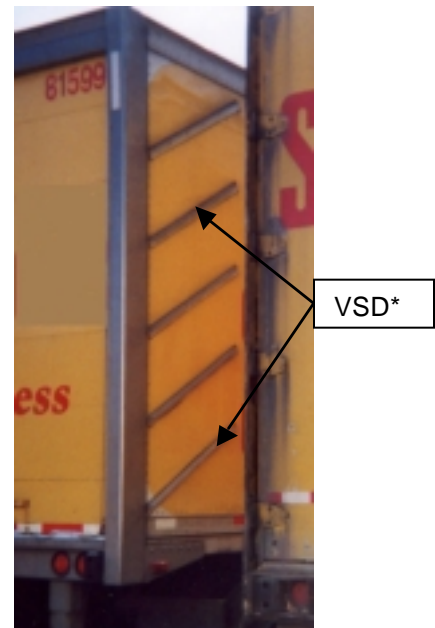
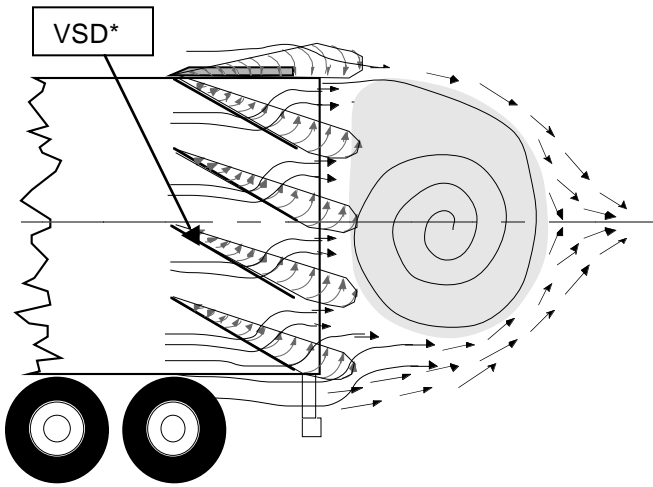


Figure 15. Sketch of a top view and a side view of the trailer base wake flow characteristics for a typical tractor-trailer truck.



***PATENT PENDING**

Figure 17. Photograph of the vortex strake trailer base treatment device installed on the aft portion of the trailer.



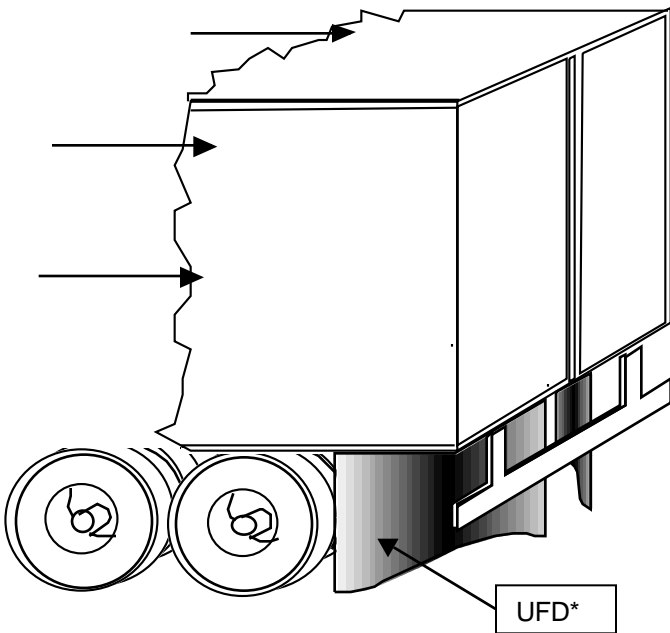
***PATENT PENDING**

Figure 18. Sketch of a side view of the vortex strake trailer base wake flow characteristics for a typical tractor-trailer truck with the base treatment installed.



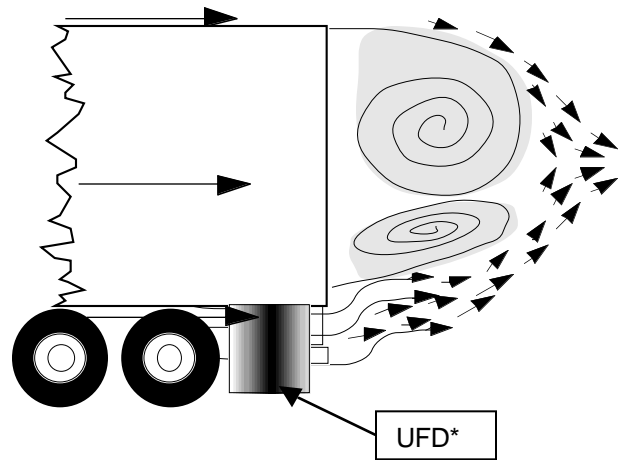
***PATENT PENDING**

Figure 20. Photograph of the undercarriage flow treatment device installed on the aft trailer undercarriage.



***PATENT PENDING**

Figure 19. Sketch of the undercarriage flow treatment device installed on the aft trailer undercarriage.



***PATENT PENDING**

Figure 21. Sketch of a side view of the trailer base wake flow characteristics for a typical tractor-trailer truck with the undercarriage treatment installed.

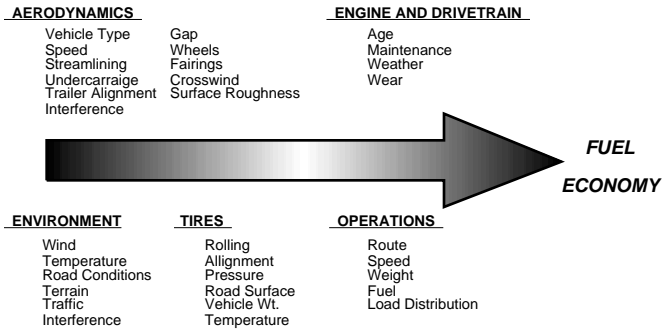


Figure 22. Operational factors that influence fuel economy of tractor-trailer trucks.

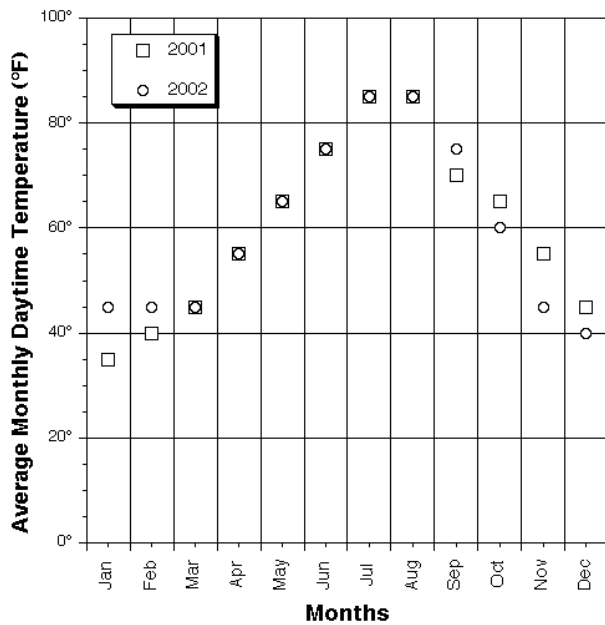


Figure 23. Plot of the average monthly daylight temperature for the years 2001 and 2002.

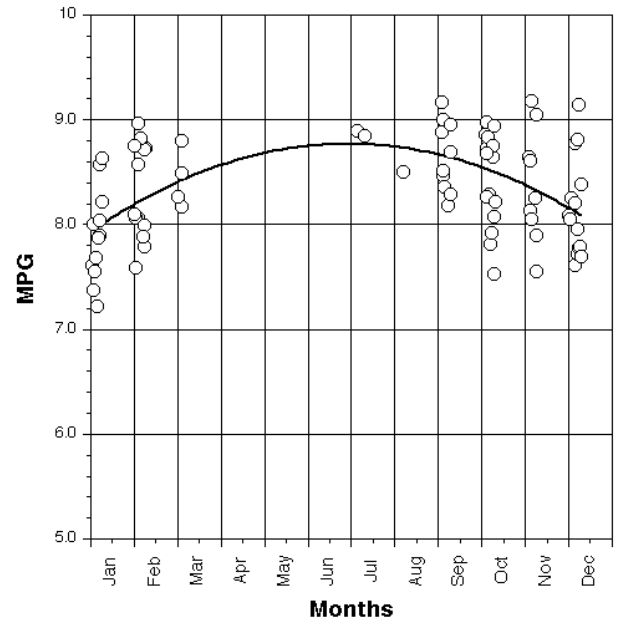
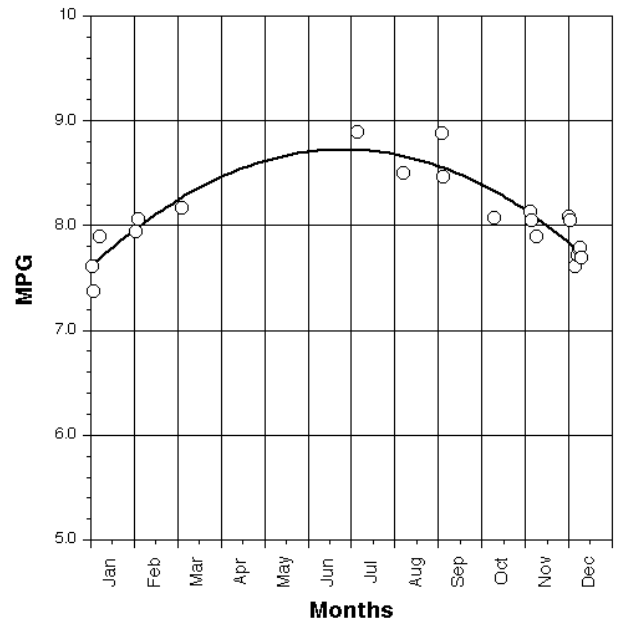
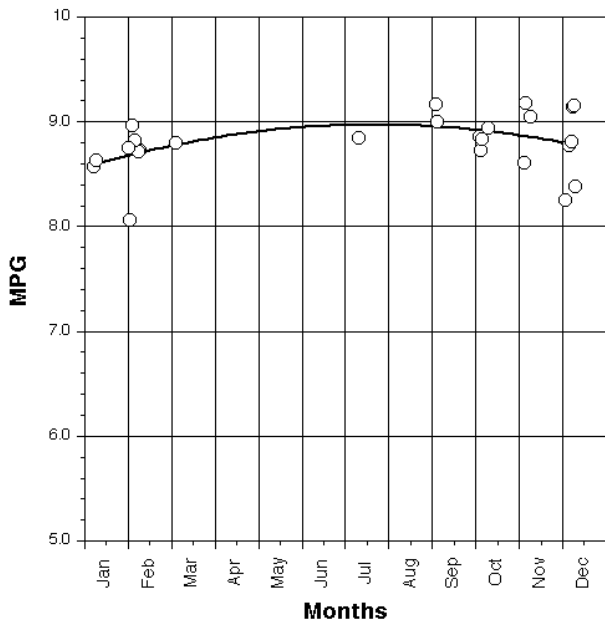


Figure 24. Plot of the individual trip fuel economy for the baseline trailers as a function of time of year.

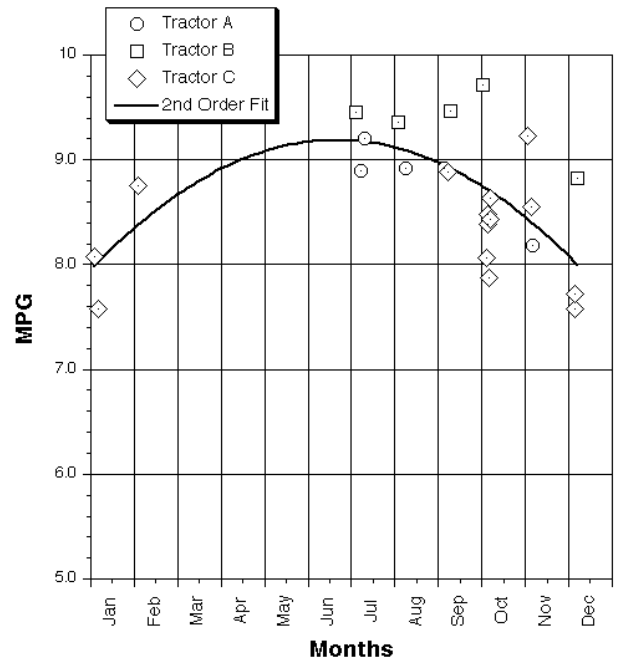


a. Tractor A

Figure 25. Plot of the individual trip fuel economy for each tractor as a function of the time of year.



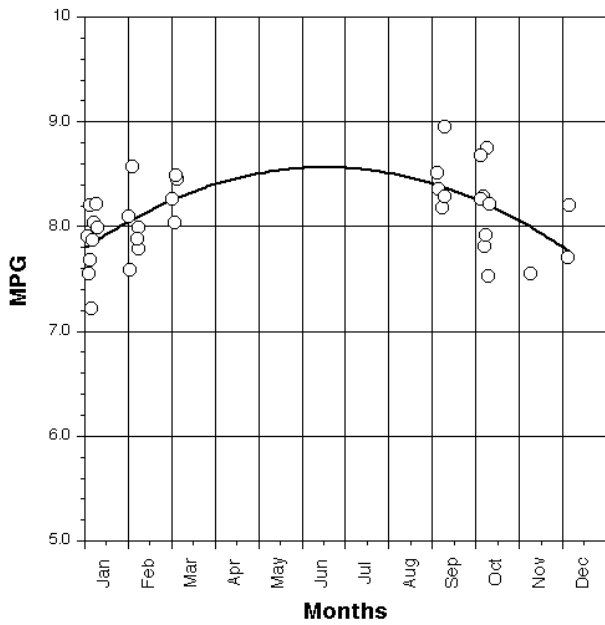
b. Tractor B



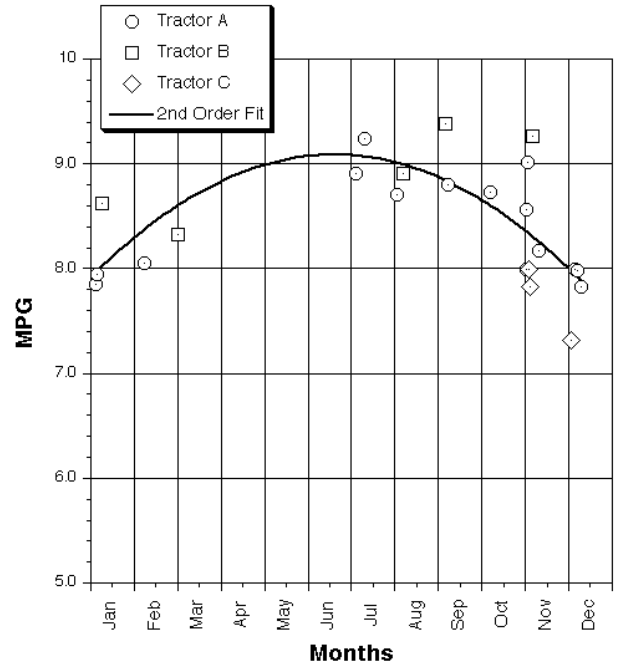
a. Crossflow Vortex Trap Device

Figure 25. continued.

Figure 26. Plot of the individual trip fuel economy for each drag reduction device as a function of the time of year.



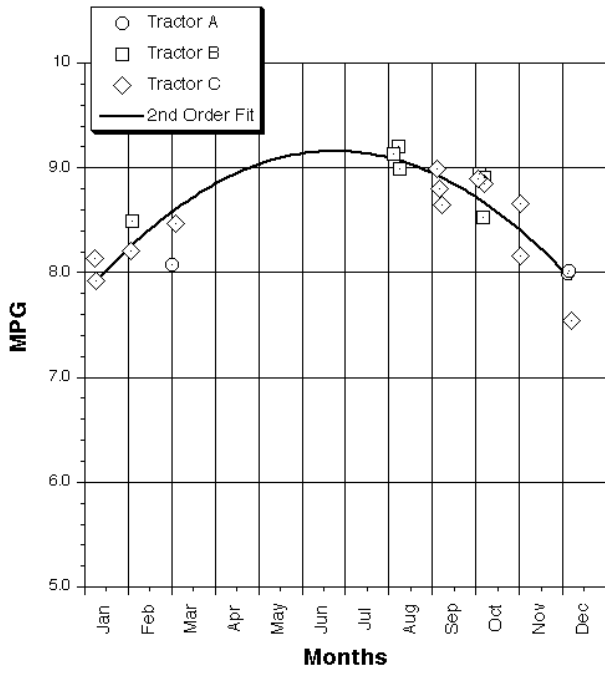
c. Tractor C



b. Undercarriage Flow Device

Figure 25. concluded.

Figure 26. continued.



c. Vortex Strake Device

Figure 26. concluded.

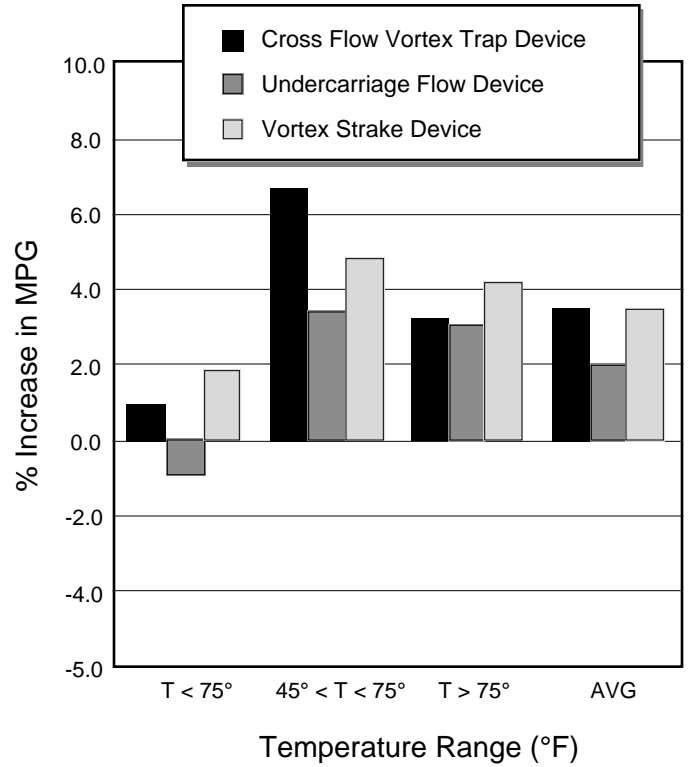


Figure 28. Average percent change in fuel economy for each drag reduction device for changes in temperature.

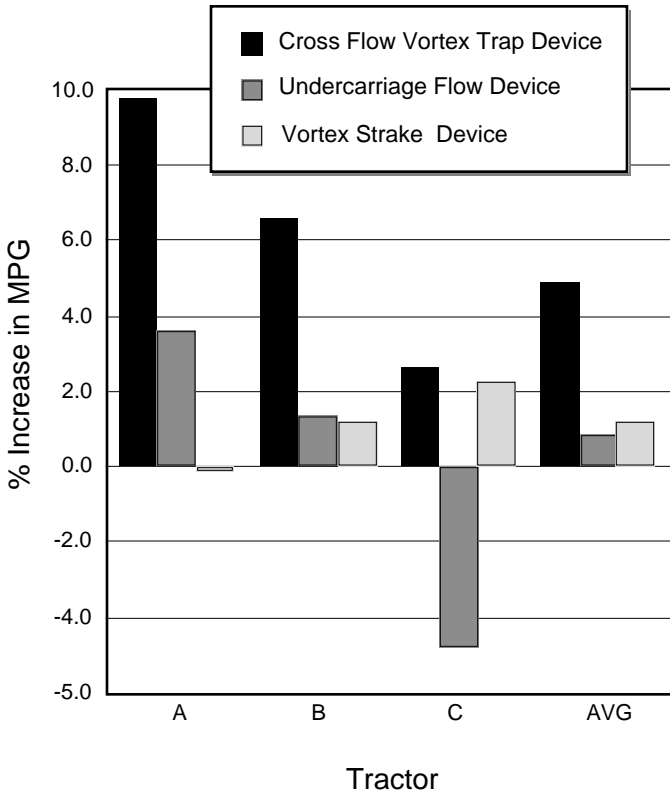


Figure 27. Average percent change in fuel economy for each combination of tractor and drag reduction device.

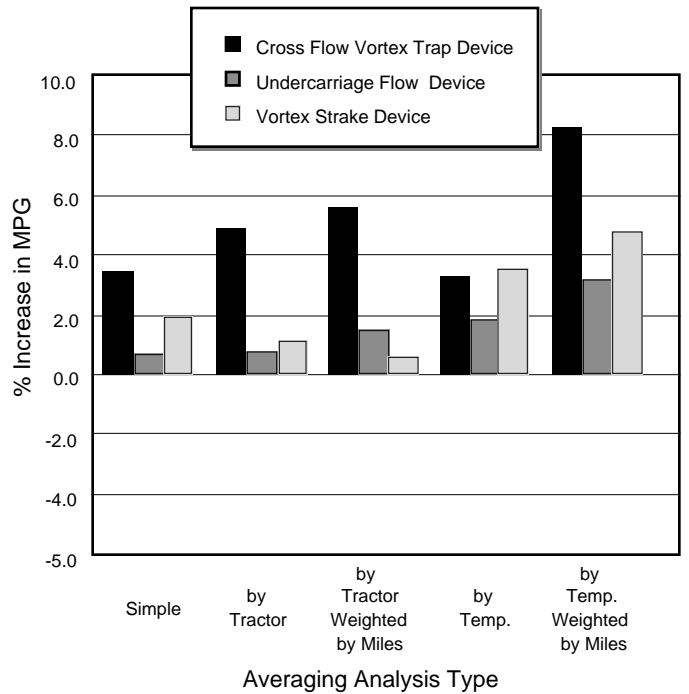


Figure 29. Percent change in fuel economy for each drag reduction device derived from a variety of data averaging and weighting approaches.

Date Printed: Thursday, October 8, 2001 1:04:17 PM

CURRENT JOB IMAGE REPORT

Cummins Engine Company INSITE Professional - CELECT Plus

Job Number: 0-010927-130240 (Image Number: 2)

Job Date: Thursday, October 8, 2001

Vehicle Unit Number: 90799

Customer:

Description:

Trip Information System

Total Fuel Used:	31069.3 gal
Total ECM Time:	6594.2 hrs
Total Engine Hours:	6594.2 hrs
Total ECM Distance:	277672.70 mi
Total Engine Distance:	277672.70 mi
ESP High Curve-Time:	0.0 hrs
Trip Fuel Used:	78.9 gal
Trip Fuel Rate:	4.75 gal
Trip MPG:	9.668 mpg
Trip Time:	16.4 hrs
Trip Distance:	762.60 mi
Trip ESP High Curve Time:	0.0 hrs
Trip ESP Distance:	0.00 mi
Trip Drive Fuel:	78.5 gal
Trip Drive MPG:	9.711 mpg
Trip Idle Fuel:	0.4 gal
Trip Idle Time:	1.0 hrs
Idle Percent Usage	6.30 %
Trip PTO Fuel:	0.0 gal
Trip PTO Time:	0.0 hrs
Trip %PTO:	0.00 %
Number of Sudden Decelerations:	0
Brake Actuation/1000 miles:	456 per 1000 mi
Trip % Distance in CC:	72.65 %
Trip % Distance at Max Speed:	0.01 %
Trip % Distance in Top Gear:	88.87 %
Trip % Distance-Direct Drive:	6.46 %
Trip % Distance-ESP Curve:	0.0 %

Table 2. Trip information listing for crossflow vortex trap device